Towards Direct Synthesis of Alane: A Predicted Defect-mediated Pathway Confirmed Experimentally

L.-L. Wang,[a] A. Herwadkar,[a] J. M. Reich,[a,b] D. D. Johnson,*[a,c,d] S. D. House,[d,e] P. Peña-Martin,[d] A. Rockett,[d] I. M. Robertson,[d,f] S. Gupta,[a] and V. K. Pecharsky*[a,c]

Abstract: Alane (AlH_3) is a unique energetic material that has not found broad practical use for over 70 years due to difficulties of its direct synthesis from elements. Using density functional theory we examine the defect-mediated formation of alane monomers on Al(111) in a two-step process: (1) dissociative adsorption of H_2 and (2) alane formation; both are endothermic on clean surface. Only with Ti-dopant to facilitate H_2 dissociation and vacancy to provide Al adatoms, both processes become exothermic. In agreement, *in situ* scanning tunnelling microscopy showed that during H_2 exposure alane monomers and clusters form primarily in the vicinity of Al vacancies and Ti atoms. Moreover, ball-milling samples of Al with Ti (providing necessary defects) showed a 10% conversion of Al into AlH_3 or closely related species at 344 bar H_2, indicating that the predicted pathway may lead to direct synthesis of alane from elements at pressures much lower than the 10^4 bar expected from bulk thermodynamics.

Introduction

With a capacity of 10.1 wt% H_2, AlH_3 (aluminum trihydride or alane) is a hydrogen-storage material that has a strong potential for practical use due to a single-step release of all available hydrogen below 100 °C.[1] The major challenge that prevents its widespread application is lack of efficient, low-cost processes for the preparation of alane on a large scale. Chemical[2-5] and mechanochemical[6-7] methods to synthesize alane from other metal hydrides have been demonstrated, but direct synthesis from the elements at moderate hydrogen pressure remains elusive. Pure Al does not react with hydrogen to form alane at room temperature unless subjected to impractically high hydrogen pressures exceeding 7 *k*bar[1, 8].

Early studies[9-13] have shown that atomic H can react with the Al(111) surface to form alane, as evidenced by products containing alane-derived species. A scanning tunneling microscopy (STM) study, supported with surface infrared measurements by Go et al[14-15] showed that the etching of Al(111) by atomic H occurs at both steps and terraces. This indicates that H_2 dissociation on the Al(111) surface must be the first step for a process that leads to the formation of alane. Transition-metal (TM) dopants, such as Ti, are known to catalyze (de)hydrogenation of $NaAlH_4$[16-17] and other metal hydrides[18-20]. Ti-dopants on Al(111)[21-24] and Al(100)[25-28] in both surface and subsurface configurations have been shown to reduce the barrier for H_2 dissociation and, especially in the former case, the barrier may become close to zero. Some studies[22, 24, 26] have proposed that subsurface Ti can be more active than surface Ti in alane formation because of the lower barrier for H-spillover to Al by avoiding the formation of strong Ti-H bonds that hinder alane formation.

However, when H-coverage is high and the surface Al can be continuously consumed, Ti tends to segregate to the surface and form a strong bond with the H. As reported by a recent study[29] of a Ti-doped Al(111) surface as a potential heterogeneous catalyst for hydrogenation reactions, it has been found that the adsorption of H and CO keeps Ti in the surface layer. On the other hand, the self-diffusion barrier for an Al adatom on Al(111) is only[30] ~0.04 eV, much smaller than the barrier for H-diffusion[24, 31] (0.15 eV), or H-spillover from subsurface Ti (0.23 eV)[22] and surface Ti (0.7 eV[24] to 0.9 eV[22]). Hence, besides H-spillover, especially for surface Ti-H* complex (* stands for an adsorption site), the availability of Al vacancies and adatoms is another substantial factor that affects the formation of alane.

The significance of vacancies and Ti atoms in alane formation should be experimentally verifiable. STM offers a unique opportunity to directly observe the surface of Al upon exposure to H_2 with atomic resolution. Alanes have been previously studied by STM, in which a bare Al(111) surface was exposed to cracked (atomic) hydrogen gas, which resulted in alane oligomer formation that could be identified by size[14-15]. However, for H-storage, it is more technologically relevant to understand the formation of alane from exposure to molecular H_2. Rather than cracking the molecular H_2 by filament, a catalyst on the surface may assist in dissociating the H_2 to enable alane formation. By preparing both bare Al and Ti-doped Al surfaces *in situ*, a pristine surface can be maintained such that one can expose these surfaces to molecular H_2 and detect the reactions as they occur, both spatially and temporally, during H_2 exposure. In particular, the ability to monitor where the reaction products

[a] Dr. L.-L. Wang, Dr. A. Herwadkar, Dr. J. M. Reich, Dr. S. Gupta, Prof. D. D. Johnson and Prof. V. K. Pecharsky
Ames Laboratory, U.S. Department of Energy
Ames, IA 50011-3020, USA
E-mail: ddj@ameslab.gov
[b] Dr. J. M. Reich
Department of Chemistry
University of Illinois Urbana-Champaign
505 South Mathews Ave., Urbana IL 61801, USA
[c] Prof. D. D. Johnson and Prof. V. K. Pecharsky
Department of Materials Science & Engineering
Iowa State University
2200H Hoover Hall, Ames, IA 50011-2300, USA
[d] Dr. S. D. House, Dr. P. Peña-Martin, Prof. D. D. Johnson, Prof. A. Rockett and Prof. I. M. Robertson
Department of Materials Science & Engineering
University of Illinois Urbana-Champaign
1304 W. Green St., Urbana, IL 61801, USA
[e] Dr. S. D. House
Department of Chemical and Petroleum Engineering
University of Pittsburgh
3700 O'Hara St., Pittsburgh, PA 15261, USA
[f] Prof. I. M. Robertson
Department of Materials Science & Engineering
University of Wisconsin-Madison
1415 Engineering Dr., Madison, WI 53706, USA

Supporting information for this article is given via a link at the end of the document.

form provides insight into the role the dopant or other surface features may play, such as terrace edges or vacancies. Al-Mahboob et al[24] employed STM to study the impact of Ti atom location on alane-forming reaction by focusing on the dissociation of H_2 and H-spillover on the Al surfaces. The Al surfaces, however, were highly stepped, with monolayer-height islands and pits. While this allowed the presence and extent of the reaction to be gauged via the etching or Ostwald ripening of these large features, it limited what understanding could be gained from the atomic-scale details involved in the process of alane formation.

In this work we examine defect-mediated formation of alane using density functional theory[32-33] (DFT) and experiment, which provides both a direct observation of the process and the environmental conditions surrounding it, as well as a deeper understanding of the energetics and reactions that occur to explain why it forms under those conditions. DFT calculations predict a point-defect-mediated formation of alane requiring Al adatoms in the presence of vacancies and Ti dopants. STM measurements on an H_2-exposed Al(111) surface show alane forms near both Al vacancies and Ti dopants, while neither alane nor Al vacancy formation occurs under the same H_2 exposure without the presence of Ti dopant, suggesting that both a vacancy and Ti dopant are necessary for alane formation. For direct confirmation, our preliminary ball-milling experiment (providing the necessary Ti dopants, Al vacancies, and adatoms) demonstrates a 10% conversion of Al into AlH_3 or AlH_3-like moiety at 344 bar H_2 in the presence of catalytic quantity Ti.

Results and Discussion

Here we first investigate the reaction energies to form alane on a pristine Al(111) surface from molecular H_2 in DFT. Equation (1) gives the two-step surface reactions, where □ stands for a vacancy and *N* for the total number of Al atoms in the slab.

$$Al_N + (3/2)H_2 = Al_N + 3H^* = Al_{N-1}\square + (AlH_3)^* \quad (1)$$

The first step is the dissociative adsorption of $(3/2)H_2$ to 3H* and the second step is the combination of 3H* with an Al adatom to form an alane molecule. The reaction diagram with energetics and atomic configurations are shown in Figure 1. The initial state (I_1) is the pristine Al(111) and $(3/2)H_2$ molecule, which are used as energy reference zero. The intermediate state (M_1) is the 3H* adsorbed on Al(111) at fcc sites. The final state (F_1) is the alane formed by etching out an Al adatom and adsorbed at the fcc site away from the vacancy. The dissociative adsorption of H_2 on the pristine Al(111) gives an energy cost of +0.58 eV for 3H*. Then forming an alane by directly etching the surface, creating both a vacancy and an Al adatom with the adatom forming alane, incurs a further, albeit small, energy cost of +0.06 eV.

$$Al_{N-1}\square + (3/2)H_2 + Al^b = Al_{N-1}\square + 3H^* + Al^b = Al_{N-1}\square + (AlH_3)^* \quad (2)$$

Next we consider the role of a vacancy without a Ti-dopant in Equation (2). If Al(111) is processed to start with a vacancy (I_2), which has an energy cost of +0.53 eV with respect to I_1 with the Al atom being removed to bulk, Al^b, (and later an Al adatom will be introduced to form alane), it can help stabilize H*. The new intermediate state (M_2) with 3H* adsorbed at the bridge sites of the micro-facets around the vacancy has an energy gain of 0.20 eV with respect to I_2. M_2 is also 0.25 eV more stable than M_1, which means that in the presence of H*, the vacancy formation on Al(111) is energetically favorable[31]. However, if these H* are used to form alane in F_2 by combining with the Al adatom from I_1, it costs 0.31 eV to do so, much higher than the 0.06 eV from M_1 to F_2. The overall surface reaction in Equation (2) is also endothermic.

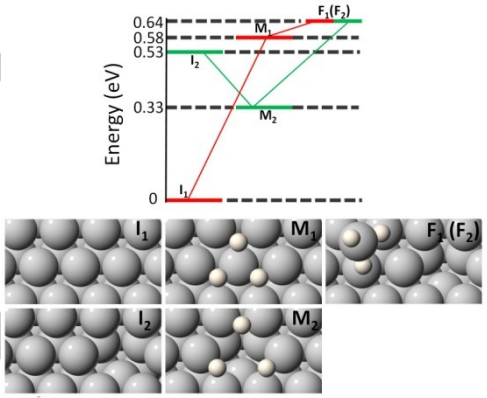

Figure 1. Reaction diagram for alane formation on pristine (Eqn (1), red) and defected (Eqn (2), green) Al(111) surfaces. (Top panel) Relative energies (eV) for initial (I), intermediate (M), and final (F) states. (Bottom panel) Atomic configurations are shown for each state on pristine (top row) and defected (bottom row) surfaces. Both reactions share the same final state. Auxiliary species H_2 and Al^b are not shown for clarity. Gray and white spheres stand for Al and H, respectively.

From Equation (1), to form alane on a clean Al(111) surface, the largest energy cost is the first step to activate H_2 to H*. Once H* are present on Al(111), the second step of direct etching to form alane only costs 0.06 eV. This agrees with experiment[14] that atomic H can etch Al(111) at both step sites as well as the terrace sites with the creation of vacancy clusters. From Equation (2), although a pre-existing vacancy can stabilize H* in Step 1, forming alane in Step 2 with an Al adatom costs a sizable 0.31 eV. Thus, processing pure Al to increase defects alone, such as with ball milling, does not favor the formation of alane.

Another way to assist the dissociation of H_2 and stabilize H* is with a TM dopant, such as Ti. A recent study[24] found that subsurface Ti can facilitate both H_2 dissociation and H-spillover to Al, while surface Ti hinders the H*-spillover. With DFT calculations, we found that a Ti-dopant prefers the subsurface substitutional site in a clean Al(111) surface to lower surface energy and enhance the favorable Ti-Al interaction. However, with the adsorption of H* and alane, the most thermodynamically stable configuration is for Ti to segregate to the surface in direct

interaction with the reactants and products (see Figure S1 and S2 in supporting information). This behavior also agrees with a recent surface infrared spectroscopy study[34] using atomic H source to investigate the effect of Ti on alane formation, where alane monomers are predominantly found and oligomerization of alane is hindered by Ti-AlH_3 interactions.

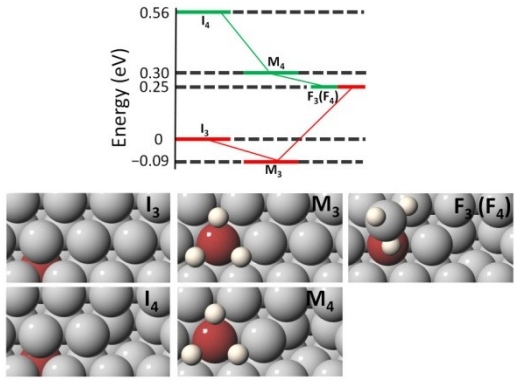

Figure 2. Reaction diagram for alane formation on Ti-doped Al(111) surface without (Eqn (3), red) and with (Eqn (4), green) Al vacancy. Relative energies of the initial (I), intermediate (M) and final (F) states are shown in the top panel and the corresponding atomic configurations are shown in the bottom panel. Both reactions share the same final states. Auxiliary species H_2 and Al^b are not shown for clarity. Gray, red and white spheres stand for Al, Ti and H, respectively.

$$Al_{N-1}Ti + (3/2)H_2 = Al_{N-1}Ti + 3H^* = Al_{N-2}Ti\square + (AlH_3)^* \quad (3)$$

For the effects of a Ti-dopant without a vacancy on alane formation, as in Equation (3) and Figure 2, the initial state of Ti occupying a subsurface site (I_3) was considered as energy zero. For the intermediate state (M_3) with 3H*, the lowest-energy configuration corresponds to 3H* sitting on the fcc sites attaching to Ti segregated to the surface, which results in an exothermic 0.09 eV for the first reaction step. For the final state (F_3) in Equation (3), an alane is formed by creating an Al vacancy, with the Al adatom diffusing to the surface Ti site and forming an alane there with 3H*. Ti still prefers to stay on the surface site to interact with alane. This second step still costs 0.34 eV to react because of creating an Al vacancy and breaking the strong Ti-H bonds, but compared to Equation (1), the overall reaction energy drops from 0.64 to 0.25 eV, with the largest energy cost also dropping from 0.58 to 0.34 eV. With a Ti-dopant but no vacancy, the two-step reaction energy diagram is similar to that with a vacancy but no Ti-dopant in Equation (2). The overall reactions are both endothermic and the largest energy cost is more than 0.3 eV. So activating Al(111) alone with either vacancy or Ti-dopant will not make the surface reaction energetically favorable to form alane.

$$Al_{N-2}Ti\square + (3/2)H_2 + Al^b = Al_{N-2}Ti\square + 3H^* + Al^b = Al_{N-2}Ti\square + (AlH3)^* \quad (4)$$

Now we consider activating Al(111) with both a Ti-dopant and a vacancy, as in Equation (4) and Figure 2. Again in the initial state (I_4) without adsorbates, Ti prefers to occupy a subsurface site. In addition, a vacancy is created in I_4 with the energy cost of 0.56 eV with respect to I_3, about the same on pure Al(111), see Figure 1. For the intermediate state (M_4) with 3H*, Ti prefers the surface instead of the subsurface site, which brings an exothermic 0.26 eV change going from I_4 to M_4. For the final state (F_4) with alane formed with the Al adatom from I_4 adsorbing on the surface Ti, there is another 0.05 eV energy gain. Besides activating Al(111) with Ti-dopant to favor H_2 dissociation, with the energy cost to activate Al in terms of vacancy and adatom being paid before the surface reaction, the second step also becomes favorable. The vacancy is at the 3rd nearest neighbor distance to Ti; the separation is about 5.7 Å as shown in Figure 2. The distance is less important than the fact that the energy cost to create an Al vacancy is already paid before hand, making Al adatom available, and then the surface reactions in both steps become exothermic. Thus to facilitate the formation of alane on Al(111), both H_2 and Al need to be activated with a co-located Ti-dopant and vacancy, respectively, because pure Al is known to be a poor absorber of molecular H_2[35-36].

For the switching of Ti between surface and subsurface sites in Figure 2, i.e. from I3/4 to M3/4, there will be a certain barrier. In fact, without H_2, although the subsurface site is more stable for Ti, the as-deposited Ti dopants are kinetically trapped at the surface sites, as observed both in our (see below) and previously reported STM experiments[21]. To account for this effect, we provide an alternative reaction diagram in Figure S3 using the surface-Ti as the initial configurations, I3t and I4t. Now the shifts from I3t/4t to M3/4 become more thermodynamically favorable than that from I3/4 to M3/4, because I3t (I4t) is 0.29 (0.19) eV higher than I3 (I4). The purpose of using I3/4, the most stable configurations, is to get the lower bound in reaction energy with Al defects included, which is the focus of our current study. Also as shown in Figure S4, with the nearby Al vacancy at 3rd nearest neighbor, the kinetic barrier for H_2 dissociation on Ti-dopant remains small (0.07 eV).

Using a free alane monomer in gas phase as reference, we also calculated the desorption/adsorption energy of the alane monomer on pure Al surface (F1(2) in Figure 1) to be 1.19 eV and the Ti-doped Al (F3(4) in Figure 2) to be 1.79 eV. In comparison, for bulk alane in α phase, the cohesive energy is 1.48 eV per formula unit in reference to the free alane monomer. Thus, once alane monomers are formed, there is always a tendency to form alane oligomers on pure Al surfaces, because oligomerization is thermodynamically favorable. On Ti-doped Al surfaces, such tendency will be weaker because of the stronger binding of alane monomers to Ti than Al sites. A quick estimate for an alane dimer with one half adsorbed on Ti and the other half on Al gives the stability about 1.49 eV, comparable to that of bulk alane. Also the energy cost to move the alane monomer away from Ti to Al site is 0.60 eV, which is comparable to the energy cost to activate Al vacancy to form alane monomers. So with Ti-dopants in Al surfaces for our proposed defect-mediated mechanism, the formation of alane oligomers can still happen.

The reaction of molecular H_2 at the Al(111) surface with and without the presence of Ti catalyst atoms was studied by STM to directly observe the process of alane formation as it occurred. Without Ti, pure Al(111) islands (see Figure S5 in supporting information) remain flat and metallic with no AlH_3 formation observed upon exposure to H_2. Figure 3 shows the Al surface following deposition of 0.02 monolayers (ML) of Ti, which appear as bright spots in the image. The apparent heights of the Ti atoms were 0.2-0.4 Å, depending on tip condition, with apparent diameters of 0.6-0.75 nm, which agrees well with previously observed and simulated[21] values corresponding to Ti trapped in first-layer substitutional positions.

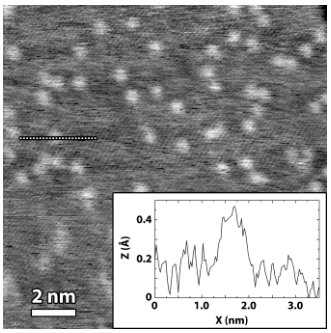

Figure 3. STM image of Al island surface showing deposited Ti (bright spots) prior to H_2 exposure. The line profile (inset) shown crosses a Ti atom (indicated by dotted line), whose apparent height matches that of a first-layer substitutional position. Scan parameters: V = 1.115 V, I = 0.208 nA.

Ti-doped surfaces were subsequently exposed to molecular H_2 for 4 hours while being scanned. Multiple islands were examined during this process, with similar behavior observed on each. Figure 4a shows the surface of one such island 108 minutes into the exposure. Ti atoms remained visible and of the same apparent heights, Figure 4b. The first noticeable change in the exposed Al-Ti surface was the appearance of topographic depressions, Figure 4c, throughout the areas examined. These features appeared as pits regardless of measurement bias polarity. These have depths of about 0.6-1.0 Å for the smaller and 0.8-1.6 Å (typically 1.1-1.4 Å) for the larger, consistent with being Al vacancies and vacancy clusters, respectively. This assignment is supported by I-V spectra taken on these pits, which reveal them to be metallic, with identical electronic behavior as the Al surface. The vacancies formed in real time during exposure to H_2, which indicates that the exposure has a role in their formation. This is consistent with previous reports of atomic H absorption by Al[9-13]. The observed vacancy cluster formation is also evidence for the proposed role of Ti in the dissociation of H_2 into atomic H, as no such vacancies were observed on the bare Al surface.

As the surface vacancies become more prevalent, bright protuberances (e.g., Figure 4d) with apparent heights greater than the Ti atoms developed. These bright features varied in size and height, with the smallest ones being about 1.2-2 Å tall, typically 1.3-1.8 Å. These apparent heights are consistent with alane monomers, as the heights lie in the range found in a previous STM study of alane by Go *et al*[14-15]. A profile along an alane monomer is shown in Figure 4d to illustrate the height and lateral extent of the feature, which are comparable to the DFT-simulated STM images (Figure S6) based on the atomic structure of F4 in Figure 2 Larger bright spots, with apparent heights typically 3-5 Å and apparent diameters around 1-2 nm, fall within observed sizes for surface alane oligomers.

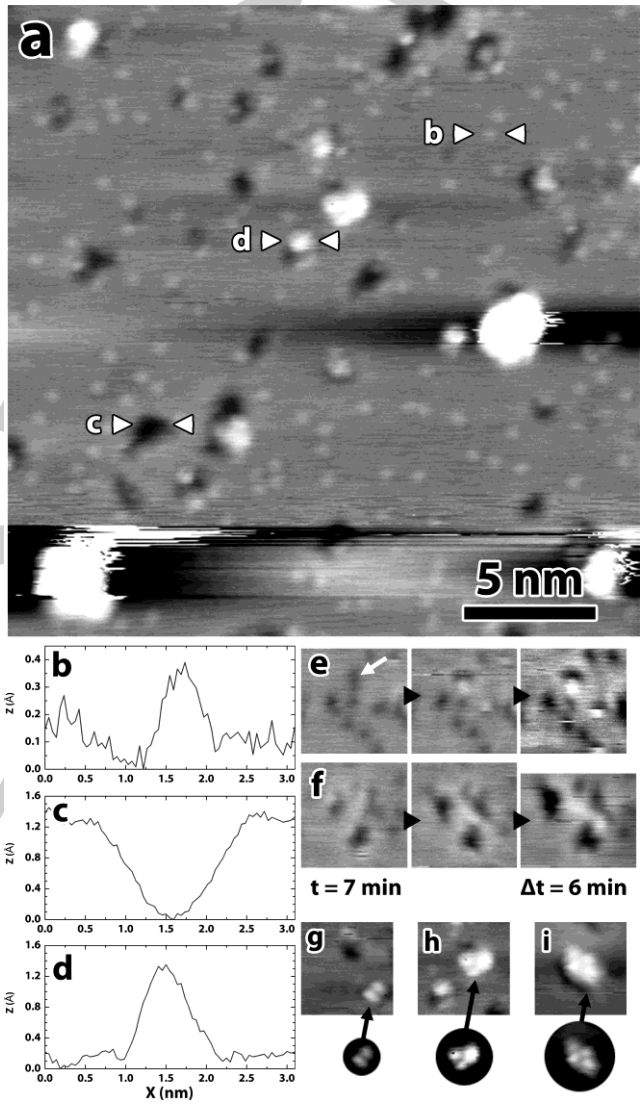

Figure 4. (a) STM scan of Al/Ti surface during exposure to 4.6×10^{-8} mbar of H_2, exhibiting the formation of vacancy cluster and alanes. Line profiles across an example (b) Ti atom, (c) vacancy cluster, and (d) alane monomer formed at a vacancy edge (between triangle pairs) are included to show relative sizes and apparent heights. (e-f) Time series of (e) an alane forming at the edge of a Ti atom (white arrow) with a nearby vacancy, and (f) a string of three alanes forming between growing vacancy clusters. 6 minutes elapsed between each image. The Ti appear recessed (dark) in these images likely due to the STM tip picking up an alane. (g-i) Images of (g) an alane monomer pair, (h) a monomer pair and dimer, and (i) an alane quartet. Circled images had their contrast adjusted for ease of viewing. Scan parameters (a) V = -1.441 V, I = 0.264 nA.

The alane monomer features were observed forming in real time during H_2 exposure in the vicinity of vacancy clusters and Ti dopants, as seen in the two time-series shown in Figures 4e-f. The first image in each series was acquired 7 minutes after dosing began, with a 6-minute interval between each subsequent image. In these images the Ti appear as shallow depressions, though the magnitude of their depth is the same as their previous height. This temporary contrast reversal is likely due to the scan tip picking up a molecule, with the contrast reverting to normal once the molecule was dropped. Such behavior has been reported while imaging surface alanes[14-15]. Despite the reversal, the Ti could still be distinguished from vacancies due to their different apparent depths. Clustering and groupings of alanes were also observed, including monomer pairs (Figure 4g-h), dimers (Figure 4h), and larger groups (Figure 4i). The tendency of the alanes to be observed located at the edges or in the close proximity of vacancies and Ti atoms is consistent with the findings presented in the previous sections about this combination being most favorable for alane formation.

Following a 2-hour post-hydrogen-exposure anneal at 100 °C, no significant topographical changes were noted. While thermal harvesting and desorption of smaller surface alanes has been observed at 85°C[14], alane monomers appeared to still be present in roughly the same quantities on the specimen, although many exhibited reduced apparent heights, typically 0.6-1 Å. One possible explanation is that these alanes may have dehydrogenated, leaving behind their Al atoms on the surface.

As described above, formation of alane on Al(111) surface becomes thermodynamically favorable starting from the I_4 state (Figure 2 and relevant discussion). Compared to the I_3 "ground" state (Figure 2), which can be easily created (e.g., by alloying Al with a few Ti at%), moving the system from the I_3 to the I_4 state requires energy input to create a vacancy and adatom. To further test the theoretical prediction, a direct mechanochemical hydrogenation of Al powder was performed in a planetary ball-mill, since defects including vacancies are formed continuously in such processes. The stored hydrogen content of the mixture after 12 hr of milling was analyzed using temperature programmed desorption (TPD), as shown in Figure 5. Nearly 1.25 wt% of hydrogen (99.8 % purity, 0.2% residual air) was released from the sample with the onset temperature close to 100 °C, typical for thermal decomposition of alane. As a control experiment, Al powder was milled with 5 wt% *h*BN under similar conditions in the absence of Ti powder. The TPD plot (Figure 5) shows only about 0.4 wt% desorption of H_2 albeit with a similar desorption profile and the onset temperature meaning that similar species are likely formed during ball milling in both cases, but the process becomes much more favorable in the presence of Ti powder. While the analysis of the phase(s) formed during the milling is difficult and still incomplete, considering a single-step desorption with low onset temperature and the published phase diagram for the Al-H system[1, 8], it is likely that AlH_3 or closely related species have formed during the ball-milling. Previous desorption studies on alane (mostly α-AlH_3) synthesized by mechanochemical metathesis reaction of $LiAlH_4$ and $AlCl_3$ and fully characterized by solid-state NMR[7] show similar desorption profile and onset temperature (see inset in Figure 5) which further suggests high likelihood that the observed H_2 desorption is from AlH_3-like moiety.

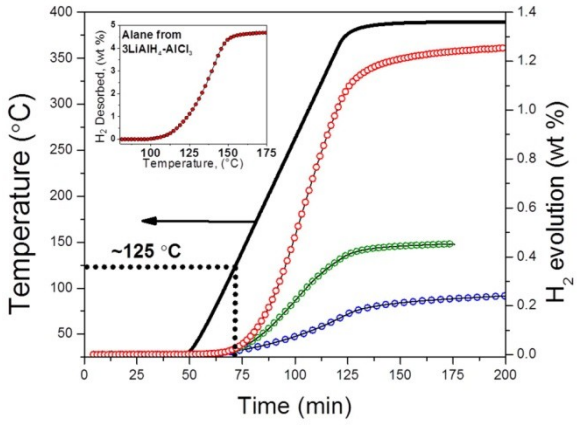

Figure 5. TPD scan of three powder samples, ball-milled under 344 bar of H_2: 75 wt.% Al + 5 wt.% Ti + 20 wt.% *h*BN (red); 95 wt.% Al + 5 wt.% *h*BN (green); and 95 wt.% *h*BN + 5 wt.% Ti (blue). Inset shows H_2 desorption profile of Alane (mostly α-AlH_3) synthesized by mechanochemical metathesis reaction of $LiAlH_4$ and $AlCl_3$ in Ref[7].

One must also consider the hydrogenation of Ti powder and *h*BN and their subsequent dehydrogenation during TPD. Given the composition of the starting mixture (~75 wt% Al, ~5 wt% Ti and ~20 wt% *h*BN), a complete mechanochemical conversion of Ti powder to stable TiH_2 and its full dehydrogenation during heating to 400 °C[37-38] is only expected to contribute 0.2 wt % H_2 which is fully consistent with the corresponding TPD data of 95 wt% *h*BN and 5 wt % Ti in Figure 5. Hence, assuming that *h*BN is an inactive process control agent, which also follows from the 95 wt% *h*BN-5 wt% Ti data of Figure 5, the results presented here indicate an approximate 10% yield of AlH_3-derived moieties in the presence of titanium under the described experimental parameters. This defect-mediated surface phenomenon is limited in yield by the formation of surface alanes near vacancies and catalyst, controlled not by bulk thermodynamics but by surface vacancy formation from ball-milling, and also affected, e.g., by cold-welding. Experimental work to characterize the products and improve yield is in progress; the results will be reported when they become available.

Conclusions

Using DFT calculations, we have studied the formation of alane monomers on Al(111) surfaces involving cooperative effects of defects (surface vacancies and catalyst) in a two-step reaction: (1) dissociative adsorption of H_2 and (2) alane formation from Al adatoms and atomic H. On pristine Al(111), both steps are endothermic, while step 1 becomes exothermic when Al(111) is activated with either vacancy or Ti-dopant. However, when Al(111) is activated with both Ti-dopant and vacancy to facilitate H_2 dissociation and provide Al adatoms,

respectively, it becomes thermodynamically favorable to form alane monomer in both steps of the surface reaction. Alane formation on the Al(111) surface during exposure to molecular hydrogen was observed *in situ* by STM, mainly at locations where Ti dopant atoms and Al vacancies were both present. The predicted cooperative point-defect-mediated route explains our STM observations, and predicts the feasibility of direct mechanochemical hydrogenation of Al. A preliminary mechanochemical experiment shows ~10% conversion of Al into AlH_3 or closely related species at 344 bar H_2 in the presence of catalytic Ti, a pressure much lower than the 10^4 bar expected from bulk thermodynamics.

Computational and Experimental Section

All DFT calculations were done with the PW91 exchange-correlation functional[39], a plane-wave basis set and projector augmented wave[40] method, as implemented in the Vienna Atomic Simulation Package (VASP)[41-42]. The calculated Al lattice constant of 4.05 Å is the same as found experimentally[43]. The Al(111) surface is modelled as a five-layer slab in a (4×4) surface supercell. All the atoms except for the bottom two layers in the slab (fixed at bulk positions) are relaxed till the absolute values of forces are below 0.02 eV/Å. A kinetic energy cutoff of 280 eV for the plane wave basis set and a (7×7×1) Monkhorst-Pack[44] *k*-point mesh including Γ point with a Gaussian smearing of 0.1 eV have been used. Ti coverage is 1/16 or 0.06 ML. The separation between the Ti-dopant and its periodic image is 11.4 Å, large enough to treat the Ti-dopant as an isolated impurity without dopant-dopant interaction. The effects of dopant coverage and dopant-dopant interactions, such as Ti dimers, clusters, and short-range ordering in a dilute Ti-Al alloy will all be interesting problems to consider in the future, but these issues are out of scope of the current study, which focuses on the joint effect of a Ti-dopant to dissociate H_2 and an Al vacancy to provide Al to form alane. Through DFT simulations involving point defects, we calculated the surface reaction energies to form alane monomers for different Al(111) surface scenarios: pristine surface, or surface with a vacancy (and Al adatom), with a Ti dopant, or with both a vacancy (and Al adatom) and a Ti dopant, as occurs during ball-milling.[45]. The surface reaction is divided into two steps: (1) Dissociative adsorption of $(3/2)H_2$ to 3H*; and (2) 3H* combines with an Al adatom to form alane. Thermal annealing with *ab initio* molecular dynamics (MD)[46] was used to search for the most stable configurations on the surfaces. Different configurations of Ti-dopant occupying surface and subsurface sites along with various alane adsorption orientations on Al(111) were investigated. Only by activating Ti-doped Al(111) with an Al vacancy and adatom is the surface reaction exothermic for alane formation and the dissociation of H_2, which explains our STM results, as well as delineates a pathway toward the direct synthesis of alane from Al at reasonably low H_2 pressure using ball-milling.

All sample preparation and microscopy experiments for STM were carried out in an Omicron variable-temperature, ultra-high vacuum STM with a base pressure of 2×10^{-12} mbar and equipped with residual gas analyzer (RGA). All scans and spectra were taken at room temperature using a commercial platinum-iridium tip. To produce clean, flat regions of Al that were oxide and impurity free, Al(111) was grown epitaxially on Si(111) 7×7 surfaces, using the method reported by Hasan *et al.*[47] Substrates were cut from a *p*-Si(111) wafer (from Virginia Semiconductor) with a resistivity of 0.022-0.034 Ω-cm. The substrates were degassed for several hours at 600 °C then flashed multiple times at 1150 °C until a pristine surface exhibiting the Si(111) 7x7 reconstruction was obtained, confirmed by STM imaging. Aluminum was deposited on the Si substrates at room temperature via electron beam evaporation from a pyrolytic boron-nitride crucible for 10 minutes at a deposition rate of ~2 monolayers per minute, as previously calibrated using Rutherford backscattering measurements, to produce an Al film thickness of about 20 monolayers (ML). Following deposition, the film was annealed at 400 °C for 10 minutes to form flat-topped islands of Al. Following topographic and electronic characterization of the Al island surfaces using STM, the scanning chamber was filled with ultra-high purity molecular H_2 gas to a pressure of 5×10^{-8} mbar. The sample was exposed to this pressure for 5 hours, with images and current-voltage spectra acquired throughout this process. With dosing complete, the chamber was pumped down to 1.5×10^{-10} mbar, after which the sample was heated to 400 °C for 12 minutes to release any absorbed or adsorbed H_2. Approximately 0.02 ML of Ti was then deposited on top of the annealed Al islands at room temperature by electron beam evaporation for a 1 second duration. Surface images confirmed that the Ti coverage was ~0.02 ML. The residual H_2 pressure during deposition was 2.7×10^{-10} mbar. The sample was subsequently exposed to 4.6×10^{-8} mbar of H_2 for 4 hours. As with the Al-only surface, the Al/Ti surface was studied before, during, and after H_2 exposure. Following a final pump down of the chamber, the sample was heated to 100 °C for 2 hours to assure removal of any residual H_2.

The specimens for ball milling were synthesized using a Pulverisette 7 (Fritsch) planetary ball-mill. The high-pressure milling containers were fabricated from 316L grade stainless steel and lined with 440C hardened stainless steel to minimize wear and related sample contamination during milling. For the experiment, 0.5 g of Al powder (< 1 μm) was mixed with 0.03 g of Ti powder (~5 wt%) along with 0.13 g (~20 wt%) of hexagonal boronitride (*h*BN) as a process control agent. Eleven hardened steel balls (~1/2 in. dia.) weighing 8.3 g each were added to the container – with an internal volume of 5.62 in^3 (~92 ml) – yielding a powder-to-ball ratio close to 1:140. The container was sealed in an argon-filled glove box and later purged with zero-grade H_2 (Linweld, 99.999%) before pressurizing to 5000 psi (344 bar). Milling was carried out at 250 rpm for 12 h. The milling sequence alternated between forward and reverse directions for 10 min each with an intermittent pause of 5 min to keep the average temperature in the vial as close to room temperature as possible. The sample mixture obtained after 12 h of milling was analyzed for hydrogen content by temperature programmed desorption (TPD) analysis. A 200 mg sample extracted from the vial was heated in an autoclave attached to the PCTPro2000, a commercially built Sieverts type apparatus for gas volumetric measurements.

Acknowledgements

Our work was supported by the U.S. Department of Energy (DOE), Office of Science, Basic Energy Sciences. DOE Materials Science and Engineering Division supported the defect-mediated reaction studies and mechanochemistry experiments at Ames Laboratory (Complex Hydrides FWP). Ames Laboratory is operated for the U.S. DOE by Iowa State University under contract DE-AC02-07CH11358. STM experiments (SDH, PPM, AR, IMR) were supported under contract DEFC36-05GO15064 through the Sandia Metal-Hydride Center of Excellence. STM experiments were *carried out in the Frederick Seitz Materials Research Laboratory Central Research Facilities, University of Illinois. We also wish to acknowledge Vania Petrova for her assistance with operating*

the STM. DOE Chemical Sciences, Geosciences, and Biosciences Division supported the early catalytic-defect studies at the University of Illinois (LLW, DDJ) under contract DE-FG02-03ER15476 in collaboration with Ralph Nuzzo.

Keywords: alane • catalysis• DFT• STM• ball-milling

[1] J. Graetz, *Chem Soc Rev* **2009**, *38*, 73-82.
[2] A. E. Finholt, A. C. Bond, H. I. Schlesinger, *J Am Chem Soc* **1947**, *69*, 1199-1203.
[3] E. C. Ashby, J. R. Sanders, P. Claudy, R. Schwartz, *J Am Chem Soc* **1973**, *95*, 6485-6486.
[4] F. M. Brower, N. E. Matzek, P. F. Reigler, H. W. Rinn, C. B. Roberts, D. L. Schmidt, J. A. Snover, K. Terada, *J Am Chem Soc* **1976**, *98*, 2450-2453.
[5] J. Graetz, J. J. Reilly, *J Phys Chem B* **2005**, *109*, 22181-22185.
[6] H. W. Brinks, A. Istad-Lem, B. C. Hauback, *J Phys Chem B* **2006**, *110*, 25833-25837.
[7] S. Gupta, T. Kobayashi, I. Z. Hlova, J. F. Goldston, M. Pruski, V. K. Pecharsky, *Green Chem* **2014**, *16*, 4378-4388.
[8] S. K. Konovalov, B. M. Bulychev, *Inorg Chem* **1995**, *34*, 172-175.
[9] J. Paul, *Phys Rev B* **1988**, *37*, 6164-6174.
[10] M. Hara, K. Domen, T. Onishi, H. Nozoye, C. Nishihara, Y. Kaise, H. Shindo, *Surf Sci* **1991**, *242*, 459-463.
[11] H. Kondoh, C. Nishihara, H. Nozoye, M. Hara, K. Domen, *Chemical Physics Letters* **1991**, *187*, 466-470.
[12] H. Kondoh, M. Hara, K. Domen, H. Nozoye, *Surf Sci* **1992**, *268*, L287-L292.
[13] H. Kondoh, M. Hara, K. Domen, H. Nozoye, *Surf Sci* **1993**, *287*, 74-78.
[14] E. P. Go, K. Thuermer, J. E. Reutt-Robey, *Surf Sci* **1999**, *437*, 377-385.
[15] E. P. Go, K. Thuermer, J. E. Reutt-Robey, *J Phys Chem B* **2000**, *104*, 8507-8511.
[16] B. Bogdanovic, M. Schwickardi, *J Alloy Compd* **1997**, *253*, 1-9.
[17] T. J. Frankcombe, *Chem Rev* **2012**, *112*, 2164-2178.
[18] G. Liang, J. Huot, S. Boily, A. Van Neste, R. Schulz, *J Alloy Compd* **1999**, *292*, 247-252.
[19] L. L. Wang, D. D. Johnson, *J Phys Chem C* **2012**, *116*, 7874-7878.
[20] J. M. Reich, L. L. Wang, D. D. Johnson, *J Phys Chem C* **2014**, *118*, 6641-6649.
[21] E. Muller, E. Sutter, P. Zahl, C. V. Ciobanu, P. Sutter, *Applied Physics Letters* **2007**, *90*, 151917.
[22] J. C. Wang, Y. Du, Y. Kong, H. H. Xu, C. Jiang, Y. F. Ouyang, L. X. Sun, *Int J Hydrogen Energ* **2010**, *35*, 609-613.
[23] Q. Peng, G. Chen, L. J. Kang, H. Mizuseki, Y. Kawazoe, *Int J Hydrogen Energ* **2011**, *36*, 12742-12752.
[24] A. Al-Mahboob, E. Muller, A. Karim, J. T. Muckerman, C. V. Ciobanu, P. Sutter, *J Am Chem Soc* **2012**, *134*, 10381-10384.
[25] S. Chaudhuri, J. T. Muckerman, *J Phys Chem B* **2005**, *109*, 6952-6957.
[26] R. Stumpf, R. Bastasz, J. A. Whaley, W. P. Ellis, *Phys Rev B* **2008**, *77*, 235413.
[27] J. C. Chen, J. C. Juanes-Marcos, A. Al-Halabi, R. A. Olsen, G. J. Kroes, *J Phys Chem C* **2009**, *113*, 11027-11034.
[28] Y. Wang, F. Zhang, R. Stumpf, P. Lin, M. Y. Chou, *Phys Rev B* **2011**, *83*, 195419.
[29] I. S. Chopra, S. Chaudhuri, J. F. Veyan, Y. J. Chabal, *Nat Mater* **2011**, *10*, 884-889.
[30] R. Stumpf, M. Scheffler, *Physical Review Letters* **1994**, *72*, 254-257.
[31] R. Stumpf, *Physical Review Letters* **1997**, *78*, 4454-4457.
[32] P. Hohenberg, W. Kohn, *Phys Rev* **1964**, *136*, B864-B871.
[33] W. Kohn, L. J. Sham, *Phys Rev* **1965**, *140*, A1133-A1138.
[34] I. S. Chopra, S. Chaudhuri, J. F. Veyan, J. Graetz, Y. J. Chabal, *J Phys Chem C* **2011**, *115*, 16701-16710.
[35] B. Hammer, K. W. Jacobsen, J. K. Norskov, *Physical Review Letters* **1992**, *69*, 1971-1974.
[36] S. Chaudhuri, J. Graetz, A. Ignatov, J. J. Reilly, J. T. Muckerman, *J Am Chem Soc* **2006**, *128*, 11404-11415.
[37] Y. Chen, J. S. Williams, *J Alloy Compd* **1995**, *217*, 181-184.
[38] M. W. Ma, L. Liang, L. Wang, Y. Wang, Y. L. Cheng, B. H. Tang, W. Xiang, X. H. Tan, *Int J Hydrogen Energ* **2015**, *40*, 8926-8934.
[39] J. P. Perdew, Y. Wang, *Phys Rev B* **1992**, *45*, 13244-13249.
[40] P. E. Blochl, *Phys Rev B* **1994**, *50*, 17953-17979.
[41] G. Kresse, J. Furthmuller, *Comput Mater Sci* **1996**, *6*, 15-50.
[42] G. Kresse, J. Furthmuller, *Phys Rev B* **1996**, *54*, 11169-11186.
[43] C. Kittel, *Introduction to Solid State Physics*, 7 ed., Wiley, New York, **1996**.
[44] H. J. Monkhorst, J. D. Pack, *Phys Rev B* **1976**, *13*, 5188-5192.
[45] J. Huot, D. B. Ravnsbaek, J. Zhang, F. Cuevas, M. Latroche, T. R. Jensen, *Prog Mater Sci* **2013**, *58*, 30-75.
[46] L. L. Wang, D. D. Johnson, *Phys Rev B* **2007**, *75*, 235405.
[47] M. A. Hasan, G. Radnoczi, J. E. Sundgren, *Vacuum* **1990**, *41*, 1121-1123.

Entry for the Table of Contents (Please choose one layout)

Layout 2:

FULL PAPER

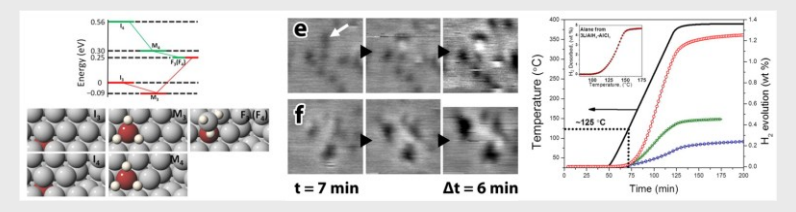

Towards Direct Synthesis of Alane: A Predicted Defect-mediated Pathway Confirmed Experimentally

Lin-Lin Wang, Aditi Herwadkar, Jason M. Reich, Duane D. Johnson, Stephen D. House, Pamela Peña-Martin, Angus Rockett, Ian M. Robertson, Shalabh Gupta, and Vitalij K. Pecharsky*

Page No. – Page No.

Title